

Iron sulfide formation on root surfaces controlled by the life cycle of wild rice (*Zizania palustris*)

Sophia LaFond-Hudson  · Nathan W. Johnson · John Pastor · Brad Dewey

Received: 16 October 2017 / Accepted: 23 August 2018
© Springer Nature Switzerland AG 2018

Abstract Iron sulfide plaques have been observed on roots of wild rice (*Zizania palustris*) and other wetland plants grown in sulfur-impacted freshwater ecosystems, but the mechanism of their formation and ramifications for plants have not been investigated. We exposed a model annual wetland plant, *Zizania palustris*, to elevated sulfate concentrations (3.1 mM) and quantified the development of iron oxide and iron sulfide precipitates on root surfaces throughout the plant life cycle. During the onset of seed production,

root surfaces amended with sulfate transitioned within 1 week from iron (hydr)oxide plaques to iron sulfide plaques. During the same week, Fe(III) decreased on roots of plants not amended with sulfate but FeS did not accumulate. Prior to FeS accumulation, sulfate-amended plants had taken up the same amount of N as unamended plants. After FeS accumulation, total plant nitrogen did not increase further on sulfate-amended plants, indicating a cessation in nitrogen uptake, whereas total plant N continued to increase in unamended plants. Sulfate-amended plants produced fewer and lighter seeds with less nitrogen than unamended plants. FeS precipitation on roots may be associated with elevated sulfide and inhibited nitrogen uptake before the end of the plant's life cycle, thus affecting the populations of this annual aquatic plant. We propose a mechanism by which a physiologically-induced decline in radial oxygen loss near the end of a plant's life cycle initiates a precipitous decline in redox potential at the root surface and in adjacent porewater, initiating accumulation of iron sulfide plaques. These plaques could be an important locus for iron sulfide accumulation in wetland sediments.

Responsible Editor: Charles T. Driscoll.

Electronic supplementary material The online version of this article (<https://doi.org/10.1007/s10533-018-0491-5>) contains supplementary material, which is available to authorized users.

S. LaFond-Hudson (✉)
Water Resource Science, University of Minnesota Duluth,
Duluth, MN 55812, USA
e-mail: lafo0062@d.umn.edu

N. W. Johnson
Department of Civil Engineering, University of
Minnesota Duluth, Duluth, MN 55812, USA
e-mail: nwjohnso@d.umn.edu

J. Pastor · B. Dewey
Department of Biology, University of Minnesota Duluth,
Duluth, MN 55812, USA
e-mail: jpastor@d.umn.edu

B. Dewey
e-mail: bdewey@d.umn.edu

Keywords Root plaques · Radial oxygen loss · Iron–sulfur cycling · *Zizania palustris* · Electron accepting buffer

Introduction

Introduction of sulfate to low-sulfate freshwater ecosystems and subsequent reduction to sulfide can induce eutrophication, enhance methylmercury production, and decimate populations of sensitive aquatic plant species (Caraco et al. 1989; Gilmour et al. 1992; Smolders et al. 2003). Field observations have correlated elevated sulfide concentrations in sediment with population declines and decreased density of some aquatic plants (Myrbo et al. 2017; Pulido et al. 2012; Smolders et al. 2003). Black iron sulfide (FeS) plaques have been observed on the roots of aquatic plants grown with elevated sulfide in several sulfur addition experiments (Gao et al. 2003; Jacq et al. 1991; Koch and Mendelssohn 1989) including our outdoor mesocosm experiment with self-perpetuating wild rice (*Zizania palustris*) populations (Pastor et al. 2017); however, little is known about conditions conducive to iron sulfide precipitation on roots and the mechanism by which it occurs.

Roots of aquatic plants create redox interfaces that are hot spots for cycling of nitrogen, sulfur, iron, and other metals (Soana et al. 2015; Schmidt et al. 2011; Lee and McNaughton 2004). Many aquatic plants transport oxygen from the atmosphere to the roots through porous tissue called aerenchyma (Armstrong and Armstrong 2005). Radial oxygen loss from roots reacts with ferrous iron in sediment to form iron (hydr)oxide plaques at the interface of the oxidized root surface and the reduced sediment (Christensen and Sand-Jensen 1998; Mendelssohn and Postek 1982; Snowden and Wheeler 1995). Together, radial oxygen loss and iron (hydr)oxide plaques provide a supply of electron accepting compounds at the root surface, hereafter referred to as an electron accepting buffer. This buffer may inhibit sulfide formation and precipitation in several ways. The release of oxygen by plant roots may reoxidize sulfide and inhibit sulfate reduction (Holmer et al. 1998). In addition, Fe(III) can oxidize sulfide, and the reduction of Fe(III) to Fe(II) may outcompete sulfate reduction (Roden and Wetzel 1996; Hansel et al. 2015). Others have observed increased FeS precipitation on roots and in sediments shortly after plant senescence (Jacq et al. 1991; Giblin and Howarth 1984), suggesting a decrease in the strength of the electron accepting buffer. However, the timing of sulfide interactions with iron on root surfaces, particularly in relation to the life cycle of the plants, remains largely unexplored.

To explore these processes, we subjected wild rice, *Zizania palustris*, an annual plant that forms large monotypic stands in the lakes and rivers of Minnesota, Wisconsin, northern Michigan, and Ontario, to enhanced sulfate concentrations. Although radial oxygen loss has not been directly quantified in wild rice, aerenchyma tissue and root surface iron oxides have been studied and documented in this species (Stover 1928; Jorgenson et al. 2012). In a previous mesocosm experiment with wild rice, increasing concentrations of porewater sulfide decreased vegetative biomass production only slightly, but strongly decreased annual seed production, leading to population declines in subsequent years (Pastor et al. 2017). Hydroponics experiments have demonstrated that sulfide reduces nutrient uptake in wetland plants (Joshi et al. 1975; Koch and Mendelssohn 1989) through inhibition of metallo-enzymes in the electron transport chain and subsequent inhibition of ATP production required for nutrient transport (Allam and Hollis 1972; Koch et al. 1990; Martin and Maricle 2015). It is not well understood why the seed production life stage of wild rice is especially vulnerable to sulfide, but decreased seed production may be associated with the timing of favorable conditions for sulfate reduction and concomitant FeS accumulation on roots.

To identify the drivers of FeS formation on the root surfaces, we tested the hypothesis that surface water sulfate loading induces FeS formation on roots. To investigate the implications of FeS root plaques for nitrogen uptake during seed production, we explored the timing of FeS formation on wild rice roots. We exposed wild rice plants to elevated surface water sulfate and quantified the speciation of iron and sulfur on root surfaces and in rooting-zone porewater during reproductive life stages. Throughout the life cycle of the plant, we also monitored growth and seed production.

Methods

Sediment was collected from Rice Portage Lake (MN Lake ID 09003700, 46.703810, – 92.682921) on the Fond du Lac Band of Lake Superior Chippewa Reservation in Carlton County, Minnesota on 5/15/15 and placed in a 400 L polyethylene stock tank (High Country Plastics) where it was homogenized by

shovel. Initial total carbon in the sediment was $14.8 \pm 1.70\%$ and initial total nitrogen was $1.12 \pm 0.13\%$ by dry weight. Eighty 4 L plastic pails were then filled with 3 L of the sediment. Each 4 L pail was placed inside a 20 L bucket that was filled with 12 L of groundwater from an on-site well to provide a 12–15 cm water column. In each pail, two seeds that were harvested in 2014 from Swamp Lake on the Grand Portage Reservation (MN Lake ID 16000900, 47.951856, – 89.856844) were planted on 5/15/15 (Julian day 135).

Forty randomly chosen buckets were amended with sulfate and forty were left unamended. On 6/3/15, the forty amended buckets received an aliquot of stock solution (5.15 g of Na_2SO_4 dissolved in 200 mL of deionized water) to result in 300 mg L^{-1} (3.1 mM) sulfate. We hereafter refer to all porewater, sediment, and plants in these buckets as “amended”. This concentration is close to the EPA secondary standard for drinking water, 250 mg L^{-1} (2.6 mM), intended to prevent laxative effects and an unpleasant taste. Although northeastern Minnesota generally has sulfate concentrations less than 10 mg L^{-1} (0.1 mM), concentrations of sulfate higher than 2.6 mM are found in some Minnesota waters, either naturally from geologic sources or from anthropogenic inputs (Myrbo et al. 2017). A sulfate concentration of 3.1 mM caused wild rice populations to go extinct within 5 years in previous mesocosm experiments with the same sediment (Pastor et al. 2017). The overlying water was sampled twice throughout the trial and re-adjusted to 3.1 mM SO_4 by adding additional Na_2SO_4 stock solution on 7/10/15. Unamended buckets had an average surface water sulfate concentration of $0.15 \pm 0.01 \text{ mM}$ when sampled on 6/23/15, consistent with the concentration of sulfate in groundwater from the on-site well. This is only slightly above observations of Moyle (1944) that wild rice grows best in waters less than 10 mg L^{-1} sulfate. We hereafter refer to all porewater, sediment, and plants in these buckets as “unamended.” Shoots were thinned on 6/23/15 to one plant per bucket. Shoot height ranged from 10 to 20 cm and the tallest, most robust shoot in each bucket was left in place.

The annual life cycle of wild rice begins with emergence from the sediment and water column in June, continues with vegetative growth in July, followed by flowering and seed production in August, and ends with the shedding of seeds and death of the

plant from late August to late September. Seeds overwinter in the sediment until they germinate in May (Grava and Raisanen 1978; Sims et al. 2012). Four plants were harvested every 2 weeks from randomly chosen amended and unamended buckets beginning at the onset of flowering (7/9/15, day 190) and continuing to the onset of seed production (8/20/15, day 232), after which plants were harvested weekly until senescence (9/22/15, day 265). The first seeds were collected on 8/20/15 (day 232) but were unripe and not yet filled. Mature seeds were not produced until 1 week after the start of seed production (day 239). On the last sample date (day 265) seeds were collected but were unfilled. Stems and leaves were no longer green, indicating that the plants had senesced. Of the four amended replicates sampled on this date, two plants did not produce seeds. Thus, “mature seed production” refers to seeds produced between Julian days 239–253.

Each plant was removed from the sediment and immediately rinsed in buckets of deoxygenated water continuously bubbled with a rapid stream of molecular nitrogen. If seeds were present, they were removed prior to sampling the plant and saved for separate analysis. While submerged in deoxygenated water, the stem was cut just above the root ball so that the shoots could be saved for mass and N analysis. The still submerged roots were then placed in jars full of deoxygenated water, which were immediately placed in a plastic bag flushed with molecular nitrogen and transported to an oxygen-free glove box (Coy Lab Products, 97.5% N_2 , 2.5% H_2). In the glove box, the roots were cleaned of sediment and all organic matter except living wild rice roots prior to removing a 1–2 g section of wet root mass for acid volatile sulfide (AVS) and iron analysis.

The plants and seeds were rinsed with deionized water and dried in paper bags for 7 days at 65°C . The dried plants were weighed, placed in polycarbonate vials with stainless steel balls, and shaken in a SPEX 800 M mixer mill until the samples were in a powdered form. Seeds were counted, weighed, and powdered using the same method. The samples were transferred to glass vials and dried again overnight at 65°C with caps loosely covering the vials. Samples were quantified for total N on an elemental analyzer coupled to a Finnigan Delta Plus XP isotope ratio monitoring mass spectrometer.

Sediment was collected at the beginning and end of the growing season. Immediately after sediment homogenization (5/15/15), five replicate samples were placed in jars and analyzed for AVS and simultaneously extracted iron. At the end of the growing season (9/22/15), a 7 cm diameter sediment core was collected from the top 10 cm of each bucket prior to root sampling. Jars were filled completely with sediment and placed in a plastic bag filled with nitrogen to prevent oxidation during transport to a glove box. In the glove box, sediment was homogenized and allocated for AVS and iron extraction.

From both sediment and roots, AVS and iron were extracted simultaneously from a 1–3 g wet sample (0.1–0.5 g dry) using 7.5 mL 1 N HCl for 4 h using a modified diffusion method (Brouwer and Murphy 1994). During a room temperature acid incubation with gentle mixing, sulfide was trapped in an inner vial containing 3 mL Sulfide Antioxidant Buffer (SAOB) and subsequently quantified using a ThermoScientific sulfide ion-selective electrode with a detection limit of 0.01 mmol L⁻¹. After the extraction, two aliquots of the 1 N HCl extracts were used for iron quantification. Ferrous iron was immediately quantified colorimetrically using the phenanthroline method on a HACH DR5000 UV–Vis spectrophotometer (Greenberg et al. 1992), and weak acid extractable iron (sum of Fe(II) + Fe(III) concentrations, hereafter referred to as “total extractable iron”) was quantified using a Varian fast sequential flame atomic absorption spectrometer with an acetylene torch.

A subset of roots was tested for chromium(II)-reducible sulfur (CRS) to determine whether AVS included all total reduced inorganic sulfur on the roots. A diffusion-based CRS method was used, which can fully extract all amorphous iron sulfide and pyrite and can partially extract elemental sulfur (Burton et al. 2008). The same sampling apparatus was used for extraction of AVS and CRS (see Burton et al. 2008 Fig. 1 for a diagram of the sampling apparatus). Chromic acid for CRS analysis was prepared according to Burton et al. (2008). Inside an oxygen-free glove box, a section of root from a plant previously analyzed for AVS was placed in the analysis bottle. An inner vial containing SAOB was also placed inside the bottle prior to sealing. Bottles were removed from the glove box and injected with chromic acid with no oxygen exposure. CRS was extracted for 48 h and quantified using a ThermoScientific sulfide ion-selective electrode.

One day prior to each root sampling date, the porewater was sampled for sulfide, sulfate, iron, and pH. First, pH was measured in situ with a ThermoScientific Orion pH electrode at a depth of 5 cm below the sediment surface and 2 cm from the stem of the wild rice plant. Porewater was collected using 5 cm length, 2 mm diameter tension lysimeter filters (Seeborg-Elverfeldt et al. 2005) (Rhizons) attached with a hypodermic needle to an evacuated, oxygen-free serum bottle sealed with a 20 mm thick butyl-rubber stopper (Bellco Glass, Inc). The entire filter end of the Rhizon was inserted vertically into the sediment just below the surface. The goal was to draw water from approximately the upper 5 cm of sediment without drawing surface water. The filter was placed with minimal jostling to avoid creating a cavity around the filter that would allow surface water to enter the sediment and contaminate the porewater. The Rhizon was placed approximately 2 cm away from the stem of the wild rice plant and on the opposite side from where pH was measured (Supplementary Fig. S1).

Porewater sulfide samples were drawn into 50-mL serum bottles preloaded with 0.2% 1 M ZnAc and 0.2% 6 M NaOH to preserve sulfide. Sulfide bottles were left to fill overnight, then stored at 4 °C in the sealed serum bottles used for sample collection for approximately 30 days before sulfide was quantified. Samples for porewater sulfate analysis were withdrawn from sulfide sampling bottles and filtered through a Dionex 1 cc metal cartridge and a 0.45 µm polyethersulfone filter approximately 3 months after they were collected. Porewater iron was collected in 8 mL serum bottles preloaded with 40% deionized water, 40% phenanthroline, 20% acetate buffer, and 1% concentrated hydrochloric acid. Iron bottles were filled until the solution turned light red, approximately 10 min. If the solution turned red before 8 mL were collected, samples were diluted with deionized water to bring the total solution to 8 mL. Iron samples were quantified within 2 h of sampling. Iron and sulfide in porewater were quantified colorimetrically using the phenanthroline and methylene blue methods, respectively, on a HACH DR5000 UV–Vis spectrophotometer (Greenberg et al. 1992). Sulfate was quantified using a Dionex ICS-1100 Integrated IC system (AS-DV Autosampler) (Greenberg et al. 1992). The saturation index was calculated to determine if the porewater was saturated with respect to iron sulfide (Eq. 1, $K_{sp} = 10^{-2.95}$)

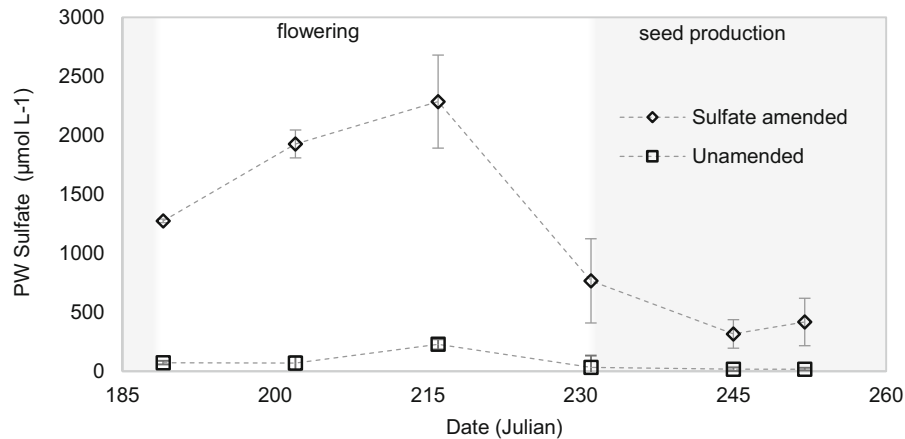


Fig. 1 Seasonal measurements of porewater sulfate concentrations 2 cm from the root surface. Diamonds depict amended plants while squares depict unamended plants. Error bars show one standard deviation around the mean. Shading represents

different life stages. Shading on left side of figure represents pre-flowering, unshaded represents flowering, and shading on right represents seed production

(Stumm and Morgan 1996). A positive saturation index indicates oversaturation and a thermodynamic force to drive precipitation, and a negative value indicates undersaturation (and potential dissolution).

$$SI = \log \frac{IAP}{K_{sp}} \text{ where } IAP = \frac{[Fe^{2+}][HS^{-}]}{[H^{+}]} \quad (1)$$

Geochemical parameters and measured attributes of plants were analyzed using repeated measures analysis of variance to determine differences between amended and unamended treatments over the course of the growing season. Analyses were performed with a repeated measures ANOVA because although individual plants were harvested on each date, each sampling date was not independent of the prior sample dates. A paired *t* test was used to determine differences between AVS and CRS concentrations on subsamples from the same roots. Analyses were performed using the statistical software SAS. Logarithmic transformations were used when data was non-normal. Data are available at the Data Repository for the University of Minnesota (<https://doi.org/10.13020/D68W98>).

Results

Porewater sulfate and sulfide

Immediately before sulfate was added to amended buckets on Julian day 154, porewater sulfate

concentrations were near $40 \mu\text{mol L}^{-1}$. By the start of flowering (day 185), sulfate concentrations in amended porewater were over $1200 \mu\text{mol L}^{-1}$, 30 times higher than the initial concentration (Fig. 1). Sulfate concentrations continued to rise for the first 30 days of flowering (until day 217), peaking at nearly $2300 \mu\text{mol L}^{-1}$. Over a 4 week period (days 217–245) surrounding the onset of seed production, sulfate concentrations in amended porewater decreased by 86% to $315 \mu\text{mol L}^{-1}$. Sulfate concentrations in unamended porewater were about $70 \mu\text{mol L}^{-1}$ at the start of flowering, roughly double the initial concentrations. Sulfate concentrations peaked at $230 \mu\text{mol L}^{-1}$ in unamended buckets on the same day as in amended buckets. During the same period that sulfate concentrations declined in amended porewater (days 217–245), sulfate concentrations in unamended buckets decreased by a similar proportion, 91%, to $20 \mu\text{mol L}^{-1}$. Porewater sulfide did not differ between amended and unamended treatments (Supplementary Fig. S2). Concentrations averaged between 1 to $5 \mu\text{mol L}^{-1}$ during flowering and increased to an average of 8– $17 \mu\text{mol L}^{-1}$ at the start of seed production. Amended rhizospheres had a higher average sulfide concentration than unamended rhizospheres during seed production, but variability was high on the days porewater sulfide was elevated. Porewater sulfide concentrations decreased near the end of seed production and rose slightly at senescence.

Acid volatile sulfur on root surfaces

When grown in sediment with sulfate-amended overlying water (3.1 mM), amended plants developed a black coating on their root surfaces by the beginning of seed production on Julian day 231 (Fig. 2). The black precipitate started just above the root ball and extended along the entire length of the roots in the sediments. Adventitious roots that grew at the surface of the sediment, however, remained white, the natural color of wild rice root tissue. Unamended plants, grown in sediment with low concentrations of sulfate in overlying water (0.15 mM), developed amber coatings characteristic of iron (hydr)oxides over the same time period.

Roots of amended plants began accumulating AVS during the flowering stage (Julian days 190–230) of the life cycle (Fig. 3a). The rate of AVS accumulation abruptly accelerated during the seed production stage (days 231–252) from



Fig. 2 Sulfate-amended (left) and unamended (right) roots. Sulfate-amended (3.1 mM sulfate in surface water) root has black color extending from about 0.5 cm above the root ball down to the tips of the roots. Unamended (0.15 mM sulfate in surface water) root has amber color characteristic of iron (hydr)oxides, especially in the 2–3 cm below root ball. The photograph was taken during senescence in October, 2014 from a pilot experiment, but color is typical of roots in this experiment. (Color figure online)

approximately $2 \mu\text{mol g}^{-1} \text{day}^{-1}$ to over $15 \mu\text{mol g}^{-1} \text{day}^{-1}$. During the seed production stage, amended roots accumulated up to 100 times more AVS than unamended roots, reaching a maximum mean concentration of $298 \pm 74 \mu\text{mol g}^{-1} \text{dw}$ at the end of seed production. In contrast, AVS on unamended roots remained at $3.2 \pm 1.7 \mu\text{mol g}^{-1} \text{dw}$ throughout the season (Fig. 3b). Between the end of seed production and final senescence (day 265), AVS concentrations on amended roots remained elevated or decreased slightly.

Although AVS concentration in amended sediment increased by one order of magnitude over the life cycle ($0.5\text{--}5 \mu\text{mol g}^{-1} \text{dw}$, Supplementary Fig. S3), sediment contained approximately 50 times less AVS per gram than the roots. Concentrations of chromium reducible sulfur on both amended and unamended roots did not differ from AVS concentrations on the same roots during seed production, indicating that crystalline forms of FeS did not make up a significant proportion of reduced sulfur (paired *t* test, $p = 0.27$, $t = 0.63$, $n = 20$).

Iron speciation on root surfaces

During flowering, concentrations of Fe(III) and Fe(II) were similar between amended and unamended roots (Fig. 3). During seed production, the redox state of iron was altered by the presence of sulfate. Concentrations of Fe(II) were much higher on amended roots compared to unamended roots ($p < 0.001$, $F = 19.1$, $df = 1, 31$), despite no significant difference in concentrations of Fe(III) between treatments. During the first week of seed production (between days 232 and 239), the concentration of ferric iron on amended roots decreased by 86%, from 233 ± 135 to $31.7 \pm 30.4 \mu\text{mol g}^{-1} \text{dw}$ while ferric iron on unamended roots decreased by 67%, from 438 ± 208 to $144 \pm 131 \mu\text{mol g}^{-1} \text{dw}$. This abrupt reduction of Fe(III) occurred the same week that the rate of net AVS accumulation increased on amended roots (Fig. 2). Following this transition, Fe(II) concentrations continued to increase (doubled) on amended roots but did not change on unamended roots.

Saturation index in porewater

Although the amended and unamended plants had significant differences in the speciation of solid-phase sulfur and iron on roots, the saturation index of FeS in the sediment porewater 2 cm away from the roots was

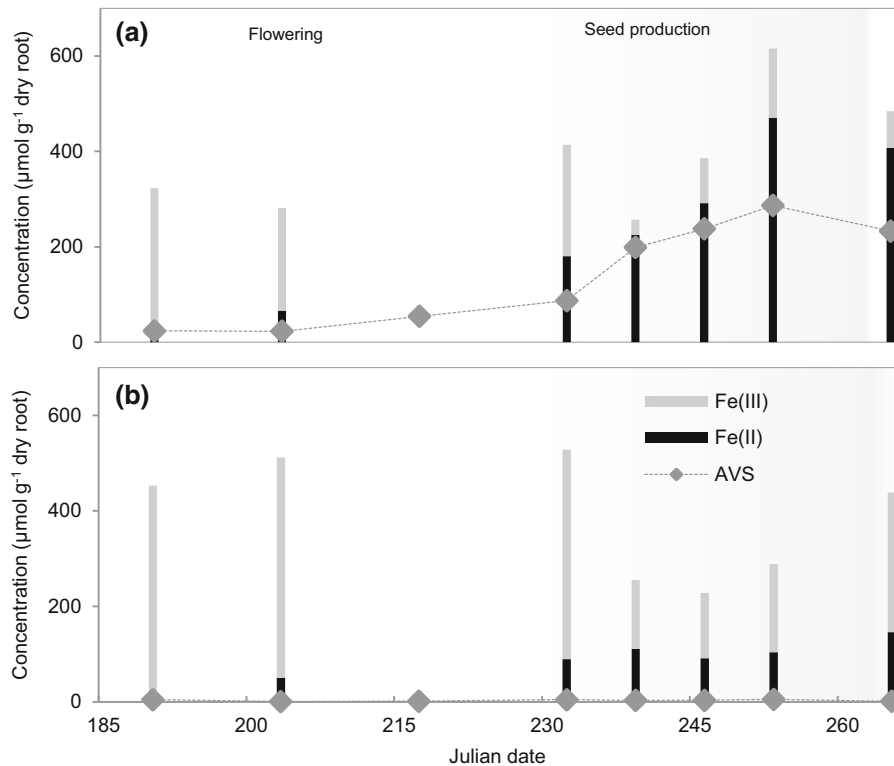


Fig. 3 Seasonal variations in iron speciation and root AVS for **a** sulfate-amended and **b** unamended conditions, and effective E_H on root surfaces. The gray bars in panels **a** and **b** indicate ferric iron and the black bars represents ferrous iron. Root AVS

concentrations are shown by gray diamonds. Error bars are omitted for clarity, but standard deviation is on average 33% of the mean

not affected significantly by sulfate amendment ($p = 0.177$, $F = 2.68$, $df = 1,4$) and remained, on average, near zero but mostly negative (-1.4 ± 0.3 to 0.1 ± 1.0) throughout the life cycle (Supplementary Table S1).

Effects on plants

The transition of plants from the vegetative growth stage to the flowering and seed production stages of the life cycle coincided with the onset of a yellowing and senescence of leaves beginning the third week of August (around day 232). Amended plants, all of which developed FeS plaques on roots, produced fewer seeds ($p = 0.067$, $F = 5.00$, $df = 1,6$, Fig. 4) with less nitrogen ($p = 0.052$, $F = 5.84$, $df = 1,6$) and smaller mass ($p = 0.069$, $F = 4.88$, $df = 1,6$). During flowering, total plant N was similar between amended and unamended plants. But, during the subsequent seed production stage, total plant N continued to

increase in the unamended plants, but not in the amended plants ($p = 0.084$, $F = 4.27$, $df = 1,6$).

Discussion

We observed rapid shifts in sulfur and iron speciation at the surface of wild rice roots during the plant life cycle that differed depending on sulfate amendment. At the onset of leaf senescence and seed production, sulfate concentrations in the porewater decreased. This was followed shortly by decreased Fe(III) concentrations on the root surface as well as increased, but highly variable, dissolved sulfide concentrations in porewater. At this stage, solid phase-sulfide increased clearly and consistently on roots of amended plants, but not on unamended plants. The rapid development of FeS plaques was concomitant with the development of fewer filled seeds with lower nitrogen contents. Total plant nitrogen continued to

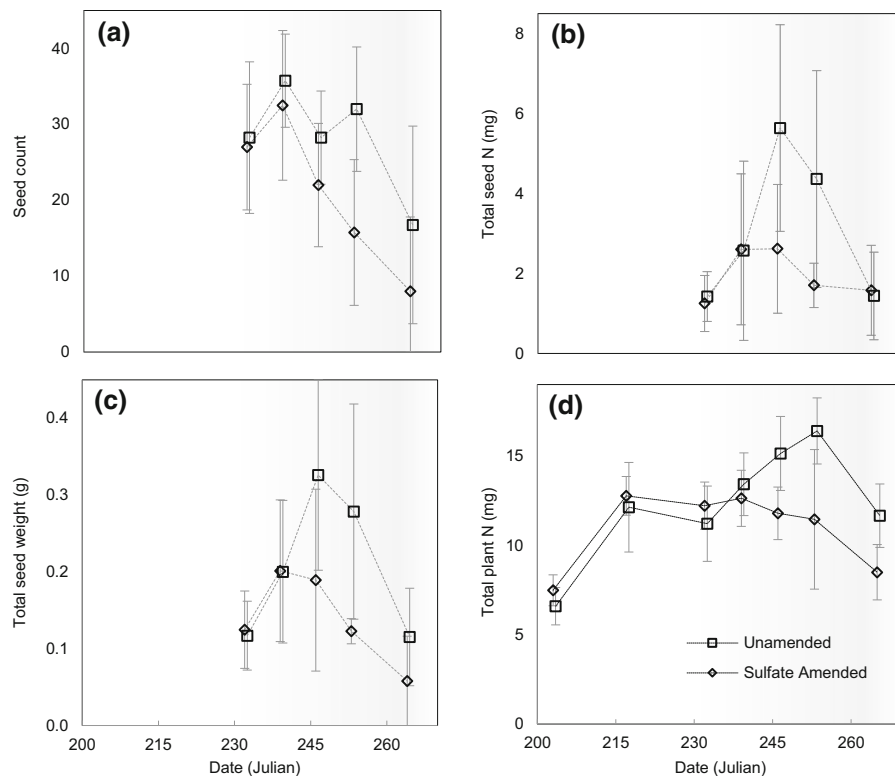


Fig. 4 Plant response in sulfate-amended and unamended conditions; **a** seed count. **b** Total seed mass. **c** Total mass of nitrogen in seeds, **d** total plant nitrogen, calculated by summing nitrogen from seeds, stems, and leaves. Diamonds represent

increase in unamended plants but not in amended plants. The strong divergence between amended and unamended plants in total plant nitrogen and precipitation of FeS suggests a feedback between sulfur biogeochemistry on or near the root surface and plant nutrient uptake.

Sulfate amendments led to more reduced conditions and a more rapid development of iron sulfide precipitate on root surfaces, clearly confirming our hypothesis that surface water sulfate induces FeS accumulation on roots. In the absence of elevated sulfate, unamended plants filled out their seeds even when redox potential declined (Fig. 3, Supplementary Fig S4). In previous experiments with self-sustaining populations of wild rice (Pastor et al. 2017), elevated sulfate had little effect on total vegetative growth of adult plants but was associated with a decrease in the number and weights of seeds produced by mature plants at the late stages of the life cycle. FeS accumulates on roots during the last stages of wild rice's life cycle in which nitrogen taken up by the plant

plants grown in surface water with 3.1 mM sulfate and squares represent unamended plants. The shaded background represents the seed production life stage. Error bars represent one standard deviation of four replicates

is allocated exclusively to panicles and seeds (Grava and Raisanen 1978; Sims et al. 2012). Porewater sulfide, which is known to decrease nitrogen uptake in plants, increased simultaneously with FeS on roots of amended plants. However, porewater sulfide was variable and increased in both amended and unamended rhizospheres, whereas FeS only increased on amended roots. Nitrogen uptake continued through the seed production phase of unamended plants but not in amended plants, which contained FeS plaques. FeS on roots may be a symptom of elevated porewater sulfide or further exacerbate its effects; our experiment was not able to distinguish between these possibilities. Regardless, the presence of root surface FeS strongly suggests that during seed production, a plant-induced reversal in the flow of electrons occurred: from a net flow of e-accepting capacity away from the root, sustaining Fe(III) in the rhizosphere, to a net flow of e-towards the root, reducing Fe(III) and introducing S(II).

The decline in nitrogen uptake and seed production concomitant with the initiation of FeS plaque precipitation on roots and porewater sulfide accumulation may explain the disproportionate effect of sulfate on seeds compared with its negligible effect on cumulative vegetative biomass prior to flowering and seed production. We suggest that plants are especially vulnerable to sulfide during seed production, because a seasonal decrease in root surface redox potential is compromised by further sulfide-induced depletion of the electron accepting buffer capacity of iron (hydr)oxides. The oxidation states of the amended and unamended root surfaces diverged during the transition from flowering to seed production (Supplementary Fig. S4), suggesting that root surface redox potential is, in part, controlled by a physiological mechanism tied to the plant's life cycle.

We hypothesize a pathway for how the living wild rice roots transition from iron (hydr)oxide plaques to iron sulfide plaques over the growing season (Fig. 5). Initially, conditions in the rooting zone are oxic, likely from radial oxygen loss (Fig. 5, stage [1]), as evidenced by precipitation of iron (hydr)oxides that accumulate equally on both amended and unamended root surfaces. At this initial stage, the root is protected from the electrons contained in sulfide and other reduced species by an ongoing supply of electron

accepting inputs, composed of both oxygen from roots and iron (hydr)oxide coatings on roots (Holmer et al. 1998; Roden and Wetzel 1996). Sulfide encountering the iron (hydr)oxide buffer is oxidized or precipitates with iron while the electron accepting buffer is maintained. In amended conditions, some of this electron accepting buffer may be consumed (Fig. 5, stage [2]) during the flowering stage, allowing dissolved sulfide to penetrate nearer to the root surface. A decrease in radial oxygen loss near the onset of seed production, as vegetative growth ceases and leaves senesce, allows dissolved sulfide to reach the root surface. Sulfide exposure may further suppress radial oxygen loss by inducing suberization, the thickening of cell walls that prevents exchange of dissolved gases across the root (Armstrong and Armstrong 2005). After radial oxygen loss is suppressed, the electron accepting buffer capacity of iron (hydr)oxides can no longer be maintained and the remaining quantity of iron (hydr)oxides is then rapidly reduced due to a net decrease in the supply of electron acceptors to the rooting zone. A decrease in radial oxygen is likely tied to the end of the vegetative growth stage of the life cycle because both the amended and the unamended root surfaces simultaneously experience a loss of Fe(III) and a decline in porewater sulfate concentrations. Concentrations of

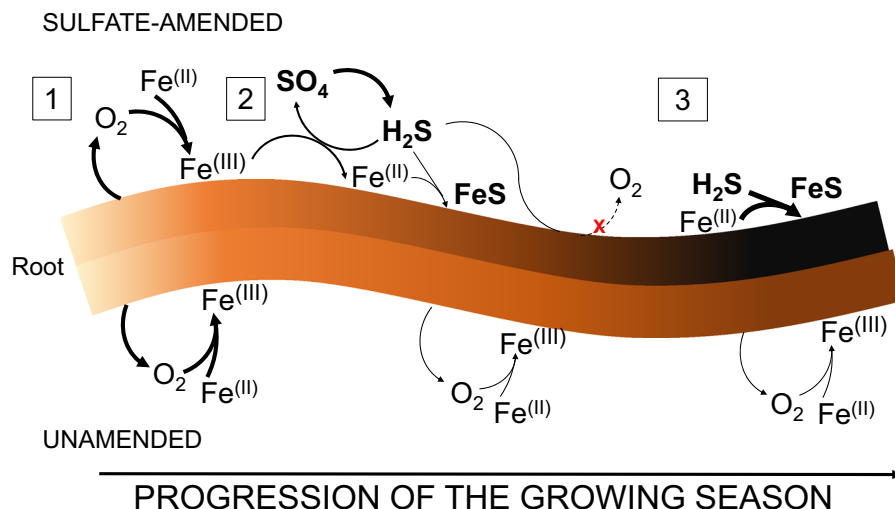


Fig. 5 Proposed mechanism of iron sulfide formation on wild rice roots exposed to elevated sulfate concentrations. Reactions depicted above the root occur on sulfate-amended root surfaces, and reactions depicted below the root occur on unamended root surfaces. Roots are protected by iron (hydr)oxides [1], but these iron (hydr)oxides are reduced by sulfide [2]. Exposure of roots to

sulfide may induce suberization, the thickening of root cell walls, which leads to decreased radial oxygen loss. Root surface anoxia accelerates the precipitation of iron sulfides [3]. In unamended roots, radial oxygen loss creates iron (hydr)oxides that remain present the entire growing season but decrease slightly in response to the life-cycle. (Color figure online)

root Fe(III) and porewater sulfate remained low in unamended plants for the rest of the growing season. But, as the amended root surface shifts toward reducing conditions, sulfide almost exclusively precipitates with reduced iron rather than being re-oxidized (Fig. 5, stage [3]). In our amended buckets, rapid accumulation of root Fe(II), root AVS, and porewater sulfide occurred within a 1–2 week period during seed production immediately following the precipitous decline of porewater sulfate and root surface Fe(III). In unamended buckets, root Fe(II) and AVS did not accumulate further, and while porewater sulfide increased, it was highly variable.

The most likely explanation for a redox transition at both the unamended and amended roots is a decrease in radial oxygen loss at the end of the vegetative growth stage when the leaves begin to senesce. Many mechanisms of rhizosphere oxidation have been described, including diffusion of atmospheric oxygen (Armstrong 1980), advection induced by temperature and vapor gradients (Dacey 1980) and Venturi-induced convection (Armstrong et al. 1992). Several studies have observed a correlation between light and rhizosphere oxygenation on diurnal time scales (Lee and Dunton 2000; Pedersen et al. 2004; Jensen et al. 2005), suggesting that some, if not most, radial oxygen loss may be photosynthetically derived. It has been previously suggested that accumulation of FeS occurs on white rice (*Oryza sativa*) roots only after plant senescence because dead roots no longer oxidize the rhizosphere (Jacq et al. 1991). However, as the plant approaches senescence, oxygen transport to the roots may decrease due to lower photosynthesis rates, subsequently slowing the regeneration of the electron accepting buffer of the root surface (Biswas and Choudhuri 1980). We observed a decrease in redox around the time that plants started to yellow and show early signs of senescence, consistent with a life-cycle-induced decline in radial oxygen loss.

Despite the rapid accumulation of FeS on roots in amended plants, the saturation index in sediment 2 cm from the roots remained relatively low, suggesting that the most severe decline in redox potential was confined to near the root surface. The Fe(II) in the FeS plaques may have come from the reduction of iron (hydr)oxides previously accumulated on the root surface. On the other hand, the sulfide in FeS plaques must have been supplied from a source external to the root. Although experimental conditions may have

impacted the timing of sulfate intrusion to the rooting zone, porewater sulfate concentrations were already well above the half saturation constant for biological sulfate reduction at the start of flowering (Pallud and Van Cappellen 2006), making it unlikely that the redox transition occurred from a delay in sulfate availability and reduction at the root surface. Once leaf senescence began, porewater sulfate concentrations ($\sim 2000 \mu\text{mol L}^{-1}$) declined by more than 80% followed by rapid accumulation of porewater sulfide (from ~ 2 to $12 \mu\text{mol L}^{-1}$) and AVS on the root surfaces ($\sim 300 \mu\text{mol g}^{-1}$). Adjacent porewater sulfide was relatively low compared to the amount of sulfur in the porewater sulfate and root AVS pools. This suggests that a large amount of sulfur passes through the porewater sulfide pool very quickly, a scenario consistent with our proposed mechanism by which sulfide near the root surface is either oxidized by the electron accepting buffer or precipitated with Fe(II). Sediment AVS ($5 \mu\text{mol g}^{-1}$) was a larger component of overall solid-phase S accumulation due to its larger mass, but did not, apparently, experience the concentrated introduction of sulfide in the same way as roots. The rapid and concentrated accumulation of iron sulfide on roots in the setting of undersaturated porewater suggests an overwhelmingly plant-dominated geochemical niche very close to the root surface.

Beyond affecting wild rice populations, the mechanism behind the rapid accumulation of FeS on roots has implications for the fate of iron and sulfide in wetland sediments. Vegetated sediment in white rice paddies (Jacq et al. 1991) and in riparian wetlands containing *Phragmites australis* and *Zizania latifolia* (Choi et al. 2006) has higher concentrations of FeS than non-vegetated sediment. Significant accumulation of FeS on white rice roots has been observed after senescence (Jacq et al. 1991), likely because decaying root material stimulates iron and sulfate reduction. When roots coated with FeS decompose, the FeS becomes incorporated into the bulk sediment. Due to the concentrated introduction of both electron donors and acceptors to the subsurface, each generation of an annual plant is effectively a “pump” for the incorporation of FeS precipitate into the sediment. In dense stands of aquatic plants, annual contributions of FeS from roots could significantly alter the geochemistry of the sediment within years to decades. If FeS plaques occur concomitantly with population declines in

wetland plants, the plant-induced sulfur pump may only last a few generations but would have implications for changes in species composition in wetland plant communities. Understanding the rates of the distinctly plant-induced sulfur pump and the short- and long-term interactions of near-root processes with bulk sediment could help to predict how the distribution of wetland vegetation and sulfur accumulation change in response to a perturbation in surface water sulfate concentrations.

The results of this study may provide a mechanistic link between observed sulfide toxicity in lab hydroponic experiments (Koch et al. 1990; Koch and Mendelssohn 1989; Pastor et al. 2017) and empirical evidence of sulfur-induced population declines of wetland plants (Lamers et al. 2002; Myrbo et al. 2017; Pastor et al. 2017; Pulido et al. 2012; Smolders et al. 2003). Our observation that sulfur cycling is altered *during* the life cycle rather than after senescence allows for the possibility of rapid feedbacks between sediment and porewater geochemistry on the one hand and annual plant populations on the other. Understanding the timing of when electron accepting buffers are present or absent and how that correlates with the plant life cycle can provide insight into how populations of wild rice and other aquatic plant species will respond to perturbations in sulfur loading to ecosystems.

Acknowledgements This research was funded by Minnesota Sea Grant and Fond du Lac Band of Lake Superior Chippewa. Sediment was provided from a wild rice lake on the Fond du Lac Reservation.

Author contributions SL-H and BD collected and analyzed samples. SL-H performed statistical analyses with guidance from JP. All authors contributed to interpreting the data and writing the manuscript.

Compliance with ethical standards

Conflict of interest The authors declare no competing financial interests.

References

- Allam A, Hollis J (1972) Sulfide inhibition of oxidases in rice roots. *Phytopathology* 62:634–639
- Armstrong W (1980) Aeration in higher plants. In: Andrews JH, Tommerup IC (eds) *Advances in botanical research*. Academic Press, Boca Raton, pp 225–332
- Armstrong J, Armstrong W (2005) Rice: sulfide-induced barriers to root radial oxygen loss, Fe²⁺ and water uptake, and lateral root emergence. *Ann Bot* 96:625–638. <https://doi.org/10.1093/aob/mci215>
- Armstrong J, Armstrong W, Beckett P (1992) *Phragmites australis*: venturi and humidity induced pressure flows enhance rhizome aeration and rhizosphere oxidation. *New Phytol* 120(2):197–207
- Biswas AK, Choudhuri MA (1980) Mechanism of monocarpic senescence in rice. *Plant Physiol* 65:340
- Brouwer H, Murphy T (1994) Diffusion method for the determination of acid-volatile sulfides (Avs) in sediment. *Environ Toxicol Chem* 13(8):1273–1275. [https://doi.org/10.1897/1552-8618\(1994\)13\[1273:DMFTDO\]2.0.CO;2](https://doi.org/10.1897/1552-8618(1994)13[1273:DMFTDO]2.0.CO;2)
- Burton ED, Sullivan LA, Bush RT, Johnston SG, Keene AF (2008) A simple and inexpensive chromium-reducible sulfur method for acid-sulfate soils. *Appl Geochem* 23:2759–2766. <https://doi.org/10.1016/j.apgeochem.2008.07.007>
- Caraco N, Cole J, Likens G (1989) Evidence for sulphate-controlled phosphorus release from sediments of aquatic systems. *Nature* 341(6240):316
- Choi J, Park S, Jaffe P (2006) The effect of emergent macrophytes on the dynamics of sulfur species and trace metals in wetland sediments. *Environ Pollut* 140:286–293. <https://doi.org/10.1016/j.envpol.2005.07.009>
- Christensen K, Sand-Jensen K (1998) Precipitated iron and manganese plaques restrict root uptake of phosphorus in *Lobelia dortmanna*. *Can J Bot* 76:2158–2163
- Dacey J (1980) Internal winds in water lilies: an adaptation for life in anaerobic sediments. *Science* 210(4473):1017–1019
- Gao S, Tanji K, Scardaci S (2003) Incorporating straw may induce sulfide toxicity in paddy rice. *Calif Agric* 57(2):55–59
- Giblin A, Howarth R (1984) Porewater evidence for a dynamic sedimentary iron cycle in salt marshes. *Limnol Oceanogr* 29(1):47–63
- Gilmour C, Henry E, Mitchell R (1992) Sulfate stimulation of mercury methylation in freshwater sediments. *Environ Sci Technol* 26(11):2281–2287
- Grava J, Raisanen K (1978) Growth and nutrient accumulation and distribution in wild rice. *Agron J* 70:1077–1081
- Greenberg AE, Clesceri LS, Eaton AD (1992) Standard methods for the examination of water and wastewater. American Public Health Association, Washington, DC
- Hansel C, Lentini C, Tang Y, Johnston D, Wankel S, Jardine P (2015) Dominance of sulfur-fueled iron oxide reduction in low-sulfate freshwater sediments. *ISME J* 9(11):2400
- Holmer M, Jensen HS, Christensen KK, Wigand C, Andersen FØ (1998) Sulfate reduction in lake sediments inhabited by the isoetid macrophytes *Littorella uniflora* and *Isoetes lacustris*. *Aquat Bot* 60:307–324
- Jacq VA, Prade K, Ottow JCG (1991) Iron sulphide accumulation in the rhizosphere of wetland rice (*Oryza sativa* L.) as the result of microbial activities. *Dev Geochem* 6:453–468
- Jensen S, Kühl M, Glud R, Jørgensen L, Priemé A (2005) Oxidic microzones and radial oxygen loss from roots of *Zostera marina*. *Mar Ecol Prog Ser* 293:49–58
- Jørgensen K, Lee P, Kanavillil N (2012) Ecological relationships of wild rice, *Zizania* spp. 11. Electron microscopy

- study of iron plaques on the roots of northern wild rice (*Zizania palustris*). *Botany* 91(3):189–201
- Joshi M, Ibrahim I, Hollis J (1975) Hydrogen sulfide: effects on the physiology of rice plants and relation to straighthead disease. *Phytopathology* 65:1165–1170
- Koch MS, Mendelssohn I (1989) Sulphide as a soil phytotoxin: differential responses in two marsh species. *J Ecol* 77(2):565–578
- Koch MS, Mendelssohn IA, McKee KL (1990) Mechanism for the hydrogen sulfide-induced growth limitation in wetland macrophytes. *Limnol Oceanogr* 35(2):399–408
- Lamers L, Falla S, Samborska E, van Dulken L, van Hengstum G, Roelofs J (2002) Factors controlling the extent of eutrophication and toxicity in sulfate-polluted freshwater wetlands. *Limnol Oceanogr* 47(2):585–593
- Lee K, Dunton KH (2000) Diurnal changes in pore water sulfide concentrations in the seagrass *Thalassia testudinum* beds: the effects of seagrasses on sulfide dynamics. *J Exp Mar Biol Ecol* 255:201–214
- Lee PF, McNaughton KA (2004) Macrophyte induced micro-chemical changes in the water column of a northern Boreal Lake. *Hydrobiologia* 522(1–3):207–220
- Martin NM, Maricle BR (2015) Species-specific enzymatic tolerance of sulfide toxicity in plant roots. *Plant Physiol Biochem* 88:36–41. <https://doi.org/10.1016/j.plaphy.2015.01.007>
- Mendelssohn IA, Postek MT (1982) Elemental analysis of deposits on the roots of *Spartina alterniflora* Loisel. *Am J Bot* 69(6):904–912
- Moyle J (1944) Wild rice in Minnesota. *J Wildl Manag* 8(3):177–184
- Myrbo A, Swain EB, Engstrom DR, Coleman Wasik J, Brenner J, Dykhuizen Shore M, Blaha G (2017) Sulfide generated by sulfate reduction is a primary controller of the occurrence of wild rice (*Zizania palustris*) in shallow aquatic ecosystems. *J Geophys Res* 122(11):2736–2753
- Pallud C, Van Cappellen P (2006) Kinetics of microbial sulfate reduction in estuarine sediments. *Geochim Cosmochim Acta* 70(5):1148–1162
- Pastor J, Dewey B, Johnson NW, Swain EB, Monson P, Peters EB, Myrbo A (2017) Effects of sulfate and sulfide on the life cycle of *Zizania palustris* in hydroponic and mesocosm experiments. *Ecol Appl* 27(1):321–336
- Pedersen O, Binzer T, Borum J (2004) Sulphide intrusion in eelgrass (*Zostera marina* L.). *Plant Cell Environ* 27(5):595–602
- Pulido C, Keijsers DJ, Lucassen EC, Pedersen O, Roelofs JG (2012) Elevated alkalinity and sulfate adversely affect the aquatic macrophyte *Lobelia dortmanna*. *Aquat Ecol* 46:283–295
- Roden EE, Wetzel RG (1996) Organic carbon oxidation and suppression of methane production by microbial Fe(III) oxide reduction in vegetated and unvegetated freshwater wetland sediments. *Limnol Oceanogr* 41(8):1733–1748
- Schmidt H, Eickhorst T, Tippkoetter R (2011) Monitoring of root growth and redox conditions in paddy soil rhizotrons by redox electrodes and image analysis. *Plant Soil* 341:221–232. <https://doi.org/10.1007/s11104-010-0637-2>
- Seeberg-Elverfeldt J, Schlüter M, Feseker T, Kölling M (2005) Rhizon sampling of porewaters near the sediment-water interface of aquatic systems. *Limnol Oceanogr* 3(8):361–371
- Sims L, Pastor J, Lee T, Dewey B (2012) Nitrogen, phosphorus, and light effects on growth and allocation of biomass and nutrient in wild rice. *Oecologia* 170:65–76
- Smolders A, Lamers L, den Hartog C, Roelofs J (2003) Mechanisms involved in the decline of *Stratiotes aloides* L. in The Netherlands: sulphate as a key variable. *Hydrobiologia* 506(1–3):603–610. <https://doi.org/10.1023/B:HYDR.0000008551.56661.8e>
- Snowden R, Wheeler B (1995) Chemical changes in selected wetland plant species with increasing Fe supply, with specific reference to root precipitates and Fe tolerance. *New Phytol* 131:503–520. <https://doi.org/10.1111/j.1469-8137.1995.tb03087.x>
- Soana E, Naldi M, Bonaglia S, Racchetti E, Castaldelli G, Brüchert V, Viaroli P, Bartoli M (2015) Benthic nitrogen metabolism in a macrophyte meadow (*Vallisneria spiralis* L.) under increasing sedimentary organic matter loads. *Biogeochemistry* 124(1–3):387–404
- Stover E (1928) The roots of wild rice *Zizania Aquatica* L. *Ohio J Sci* 28(1):43–49
- Stumm W, Morgan JJ (1996) Chemical equilibria and rates in natural waters. *Aquatic chemistry*. Wiley, New Jersey